

**The magnetic behavior of the intermetallic compound NdMn<sub>2</sub>Ge<sub>2</sub> studied by magnetization and hyperfine interactions measurements**

B. Bosch-Santos, A. W. Carbonari, G. A. Cabrera-Pasca, R. N. Saxena, and R. S. Freitas

Citation: [Journal of Applied Physics](#) **117**, 17E304 (2015); doi: 10.1063/1.4907330

View online: <http://dx.doi.org/10.1063/1.4907330>

View Table of Contents: <http://scitation.aip.org/content/aip/journal/jap/117/17?ver=pdfcov>

Published by the [AIP Publishing](#)

---

**Articles you may be interested in**

[Magnetic behavior of LaMn<sub>2</sub>\(Si\(1-x\)Ge x\)<sub>2</sub> compounds characterized by magnetic hyperfine field measurements](#)

[J. Appl. Phys.](#) **115**, 17E124 (2014); 10.1063/1.4864439

[Competing magnetic interactions in the intermetallic compounds Pr<sub>5</sub>Ge<sub>3</sub> and Nd<sub>5</sub>Ge<sub>3</sub>](#)

[J. Appl. Phys.](#) **109**, 07A716 (2011); 10.1063/1.3556920

[Magnetization and neutron diffraction studies on Dy<sub>5</sub>Si<sub>2</sub>Ge<sub>2</sub>](#)

[J. Appl. Phys.](#) **97**, 10M314 (2005); 10.1063/1.1855646

[Structure and magnetic properties of Pr<sub>2</sub>Co<sub>17-x</sub>Mn<sub>x</sub> compounds](#)

[Appl. Phys. Lett.](#) **75**, 3850 (1999); 10.1063/1.125477

[Magnetic transitions in Tb<sub>0.7</sub>Nd<sub>0.3</sub>Mn<sub>2</sub>Ge<sub>2</sub> compound](#)

[J. Appl. Phys.](#) **83**, 6974 (1998); 10.1063/1.367692

---



**AIP** | Journal of Applied Physics

**Meet The New Deputy Editors**

 **Christian Brosseau**  **Laurie McNeil**  **Simon Phillpot**

# The magnetic behavior of the intermetallic compound $\text{NdMn}_2\text{Ge}_2$ studied by magnetization and hyperfine interactions measurements

B. Bosch-Santos,<sup>1,a)</sup> A. W. Carbonari,<sup>1</sup> G. A. Cabrera-Pasca,<sup>1</sup> R. N. Saxena,<sup>1</sup> and R. S. Freitas<sup>2</sup>

<sup>1</sup>Instituto de Pesquisas Energéticas e Nucleares, Universidade de São Paulo, 05508-000 São Paulo, Brazil

<sup>2</sup>Instituto de Física, Universidade de São Paulo, CP 66318, 05314-970 São Paulo, Brazil

(Presented 4 November 2014; received 22 September 2014; accepted 16 October 2014; published online 5 February 2015)

The magnetic behavior of the intermetallic compound  $\text{NdMn}_2\text{Ge}_2$  was investigated by bulk magnetization measurements and measurements of hyperfine interactions using perturbed  $\gamma$ - $\gamma$  angular correlation (PAC) spectroscopy. Magnetization measurements indicate the presence of four magnetic transitions associated with the Mn and Nd magnetic sublattices. At high temperatures, magnetic measurements show a change in the slope of the magnetization due to an antiferromagnetic transition around  $T_N \sim 425$  K and a well defined ferromagnetic transition at  $T_C \sim 320$  K. Moreover, at  $\sim 210$  K a peak is observed in the magnetization curve, which is assigned to the reorientation of the Mn spin, and at  $\sim 25$  K an increase in the magnetic moment is also observed, which is ascribed to the ordering of Nd ions. PAC measurements using  $^{140}\text{La}$  ( $^{140}\text{Ce}$ ) and  $^{111}\text{In}$  ( $^{111}\text{Cd}$ ) probe nuclei allowed the determination of the temperature dependence of the magnetic hyperfine field ( $B_{hf}$ ) at Nd and Mn sites, respectively. PAC results with  $^{111}\text{Cd}$  probe nuclei at Mn sites show that the dependence of  $B_{hf}$  with temperature follows the expected behavior for the host magnetization associated with the magnetic ordering of Mn ions. From these results, the antiferromagnetic transition followed by a ferromagnetic ordering is clearly observed. PAC results with  $^{140}\text{Ce}$  probe nuclei at Nd sites, however, showed a strong deviation from the Brillouin function, which is attributed to the Ce 4f-electron contribution to  $B_{hf}$ . © 2015 AIP Publishing LLC. [<http://dx.doi.org/10.1063/1.4907330>]

## I. INTRODUCTION

The compound  $\text{NdMn}_2\text{Ge}_2$  crystallizes in the  $\text{ThCr}_2\text{Si}_2$  prototype structure with  $I4/mmm$  space group.<sup>1</sup> The magnetic properties of  $\text{NdMn}_2\text{Si}_2$  have been studied by neutron diffraction, magnetization, and resistivity measurements on polycrystalline samples. These studies have shown multiple magnetic transitions, making this compound a member of a family that exhibits a range of interesting magnetic properties.  $\text{NdMn}_2\text{Ge}_2$  exhibits a transition from a paramagnetic to an antiferromagnetic and then to a ferromagnetic phase in the Mn sublattice. In the ferromagnetic phase, the spins are canted with respect to the *c*-axis and below 218 K, they re-orient along the *ab*-plane continuing to be ferromagnetically coupled.<sup>2</sup> Below 23 K, an ordering of the Nd sublattice occurs with a ferromagnetic coupling in the same direction of the spins as in the Mn sublattice (*ab*-plane).<sup>2,3</sup> Other compounds in the  $\text{REMn}_2\text{Ge}_2$  family, where RE is a rare-earth element, such as  $\text{PrMn}_2\text{Ge}_2$ ,  $\text{SmMn}_2\text{Ge}_2$ ,  $\text{GdMn}_2\text{Ge}_2$ ,  $\text{DyMn}_2\text{Ge}_2$ , and  $\text{TbMn}_2\text{Ge}_2$ , also present multiple magnetic transitions.<sup>3</sup> Therefore, compounds of this family have a complex magnetic behavior that makes further local investigation necessary.

In this paper, we report a hyperfine interactions investigation of  $\text{NdMn}_2\text{Ge}_2$  with perturbed  $\gamma$ - $\gamma$  angular correlation (PAC) spectroscopy using two probe nuclei  $^{111}\text{Cd}$  and  $^{140}\text{Ce}$ , which allows the measurement of the temperature dependence of the magnetic hyperfine field ( $B_{hf}$ ) at Mn and Nd

positions, respectively. In addition, magnetization measurements were also carried out to characterize the magnetic behavior of the compound as a function of temperature. The Néel ( $T_N$ ) and the Curie ( $T_C$ ) ordering temperatures were determined by both measurements. PAC measurements using  $^{111}\text{Cd}$  probe nucleus are particularly important in  $\text{NdMn}_2\text{Ge}_2$  because the major fraction of  $^{111}\text{Cd}$  probes are found to occupy Mn sites in the crystal lattice and, consequently, such measurements can help in the determination of the spin arrangement of the Mn atoms in both, the antiferromagnetic and ferromagnetic phases, as well as making it possible to determine  $T_N$ . PAC measurements using  $^{140}\text{Ce}$  probe nuclei are also interesting first because they replace the Nd in the crystal lattice and, second, due to the small electric quadrupole moment of this nucleus. This makes it sensitive only to dipole magnetic interactions and, consequently, the measurements are free from the electric quadrupole interaction interference. Moreover, due to the arrangement of spins of the Mn atoms in the antiferromagnetic phase, the  $B_{hf}$  vanishes at Nd position. It is, therefore, possible to determine with good accuracy the Curie temperature of the ferromagnetic phase as well as to observe the changes of directions in the spins.

## II. EXPERIMENTAL PROCEDURE

Samples of  $\text{NdMn}_2\text{Ge}_2$  (Nd = 99.9%, Mn, Ge = 99.999% purity) were prepared by arc-melting the metallic components in stoichiometric proportion in argon atmosphere. A small excess of Mn, about 5 wt.%, was used to compensate evaporation

<sup>a)</sup>Electronic mail: [brianna@usp.br](mailto:brianna@usp.br).

during arc melting. After melting, the samples were encapsulated in a quartz tube under helium atmosphere at low pressure and submitted to thermal annealing at 800 °C during 24 h. Finally, samples were characterized by X-ray diffraction (XRD) and the data were analyzed by Rietveld method.

Hyperfine interactions were measured by PAC spectroscopy at the intermediate level of two gamma radiations emitted in a cascade arising from the decay of the excited states of a probe nucleus. It provides information about the hyperfine interaction between external nuclear fields and nuclear moments of probe nuclei, which are located at certain atomic sites in the crystalline structure of solid materials. The technique measures the time evolution of the  $\gamma$ -ray emission pattern caused by hyperfine interactions. A description of the method as well as details about the PAC measurements can be found elsewhere.<sup>4–6</sup> The perturbation factor  $G_{22}(t)$  of the correlation function, measured by PAC experiments, contains detailed information about the hyperfine interaction. In general, the PAC spectra are fitted by using a model that takes into account the fractional site populations ( $f$ ) and is given by the perturbation function  $R(t) = A_{22}G_{22}(t) = A_{22} \sum_i f_i G_{22}^i(t)$ , where  $A_{22}$  is the unperturbed angular correlation coefficient. Experimental measurement of  $G_{22}(t)$  allows, in the dipole magnetic interaction, the determination of the Larmor frequency  $\omega_L = \mu_N g B_{hf} / \hbar$ , where  $\mu_N$  is nuclear magneton and the calculation of the magnetic hyperfine field  $B_{hf}$  and for electric quadrupole interactions, the determination of the quadrupole frequency  $\nu_Q = eQV_{zz}/h$  as well as the asymmetry parameter  $\eta = (V_{xx} - V_{yy})/V_{zz}$ , where  $V_{xx}$ ,  $V_{yy}$ , and  $V_{zz}$  are the components of the electric field gradient (EFG) tensor in its principal axis system. Consequently, from the known nuclear quadrupole moment  $Q$ , one can calculate the major component  $V_{zz}$  of EFG and its asymmetry parameter  $\eta$ . As a consequence PAC measurements allow extracting information about the involved hyperfine parameters, as well as the characterization of structural and magnetic transitions of the crystal.

PAC measurements using  $^{111}\text{In}$  ( $^{111}\text{Cd}$ ) and  $^{140}\text{La}$  ( $^{140}\text{Ce}$ ) probe nuclei were carried out using six- and four-detector spectrometers both associated with conventional fast-slow electronic setup to measure the delayed gamma-gamma coincidences. These probe nuclei have, respectively, intermediate levels of 245 keV ( $I = 5/2^+$ ,  $T_{1/2} = 84.5$  ns, and g-factor =  $0.306 \pm 0.001$ ) for  $^{111}\text{Cd}$  and 487 keV ( $I = 4^+$ ,  $T_{1/2} = 3.4$  ns, and g-factor =  $1.014 \pm 0.038$ ) for  $^{140}\text{Ce}$ .  $\text{BaF}_2$  and  $\text{Lu}_2\text{SiO}_5$  detectors were used in the measurements with  $^{111}\text{In}$  ( $^{111}\text{Cd}$ ) and  $^{140}\text{La}$  ( $^{140}\text{Ce}$ ) probe nuclei, respectively.

For the measurements with  $^{111}\text{In}$  ( $^{111}\text{Cd}$ ) nuclear probes, a carrier-free  $^{111}\text{In}$  was deposited on a small part of the sample which was then re-melted in the arc furnace. Subsequently, the resulting ingot was sealed under helium atmosphere at low pressure in a quartz tube and annealed at 850 °C for 20 h. In the case of  $^{140}\text{La}$  ( $^{140}\text{Ce}$ ) probe, a small quantity of metallic La (replacing approximately 0.1 at. % of Nd atoms), which was previously irradiated with neutrons in the IEA-R1 reactor of IPEN to produce radioactive  $^{140}\text{La}$ , was added to the samples through arc melting followed by thermal annealing at 800 °C for 20 h also under helium atmosphere. Measurements were carried out in the temperature range 20–480 K using a closed

loop helium cryogenic system and a small furnace, respectively. For the magnetization measurements, we used a commercial Vibrating Sample Magnetometer (PPMS, QD) with an applied field of 100 Oe.

### III. RESULTS AND DISCUSSION

#### A. Structure results

The X-ray diffraction results (see Figure 1) showed the expected tetragonal structure of  $\text{ThCr}_2\text{Si}_2$  type, which belongs to the  $I4/mmm$  space group, with lattice parameters  $a = b = 4.099(1)$  Å and  $c = 10.903(3)$  Å. These values agree quite well with those of  $a = b = 4.1022(3)$  Å and  $c = 10.9085(7)$  Å previously reported<sup>7</sup> for  $\text{NdMn}_2\text{Ge}_2$ . Since the amount of radioactive  $^{111}\text{In}$  is extremely small (around  $10^{10}$  nuclei) and metal La, which contains radioactive  $^{140}\text{La}$  is of the same order of the impurity in Nd, the addition of the probe nuclei to the samples is not expected to have any influence in their structure.

#### B. PAC with $^{111}\text{Cd}$ results

Results of PAC measurements with  $^{111}\text{Cd}$  were fitted using a model where probe nuclei occupy two site fractions. The major fraction ( $\sim 90\%$ ) was modeled by a combined magnetic dipole interaction, which varies with temperature, plus a small electric quadrupole interaction, which is characterized by  $\nu_Q \sim 5$  MHz. The minor fraction presents pure electric quadrupole interaction with a broad quadrupole frequency. This quadrupole interaction is probably due to the probe nuclei at non substitutional sites. PAC measurements with  $^{140}\text{Ce}$  were fitted using a unique site fraction with a pure magnetic dipole interaction. Measured spectra for both probe nuclei are shown in Figure 2.

Figure 3 displays the temperature dependence of the magnetization ( $M$ ) and  $B_{hf}$  measured with  $^{111}\text{Cd}$  nuclei probe for  $\text{NdMn}_2\text{Ge}_2$ . The inverse of the magnetic susceptibility (inset of Fig. 3) follows the Curie-Weiss law at high temperatures and the corresponding effective magnetic moment is  $\mu_{eff} = 3.9 \mu_B$  per Mn. This value is in close agreement with

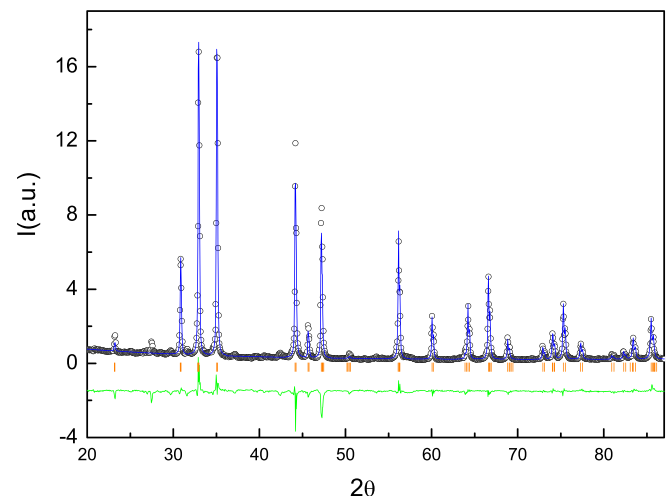


FIG. 1. X-ray diffraction pattern of  $\text{NdMn}_2\text{Ge}_2$ , which shows a single phase corresponding to tetragonal  $\text{ThCr}_2\text{Si}_2$  prototype structure.

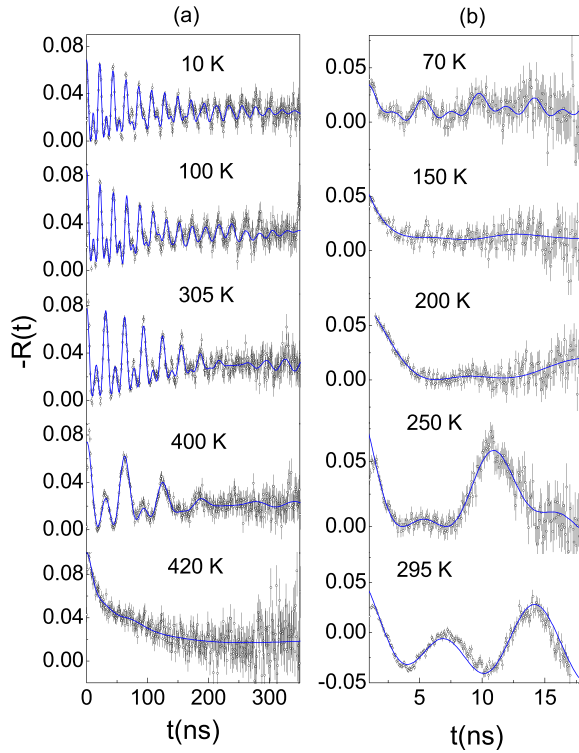


FIG. 2. Perturbation functions for  $\text{NdMn}_2\text{Ge}_2$  measured at indicated temperatures with (a)  $^{140}\text{Ce}$  and (b)  $^{111}\text{Cd}$  probe nuclei. Solid lines are the least squares fit of the theoretical functions to the experimental data.

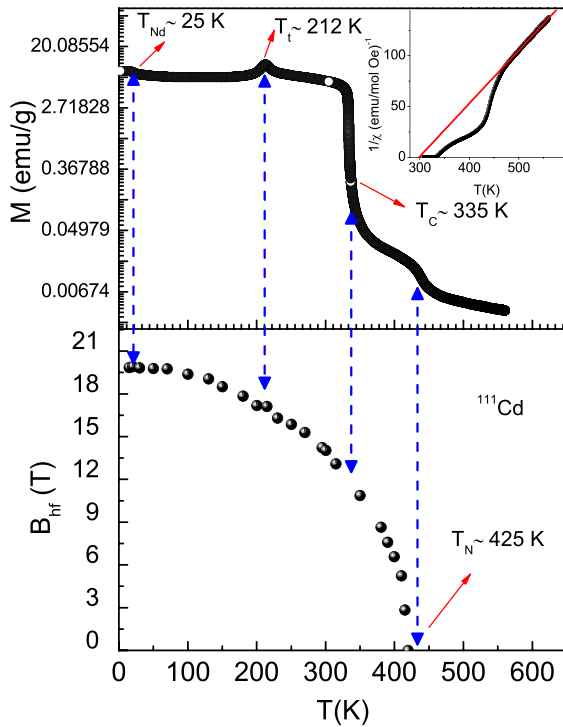


FIG. 3. Magnetization ( $M$ ) and  $B_{hf}$  at  $^{111}\text{Cd}$  probe at Mn sites as a function of temperature. Multimagnetic transitions observed with magnetization measurements are indicated by the dashed arrows. As can be seen in the figure, only the paramagnetic to antiferromagnetic transition is clearly observed by PAC measurements as well as a slight change in the  $B_{hf}$  curve at  $\sim 212\text{K}$ .

$P_{eff} = 3.5 \mu_B$  obtained for  $\text{LaMn}_2\text{Ge}_2$ .<sup>8</sup> Based on previous results,<sup>12,14</sup> it is assumed that  $^{111}\text{Cd}$  probe nuclei replace the Mn atoms in the observed major fraction. This assumption is also supported by the small value of  $\nu_Q$  as expected at the Mn position, which is much lower than those at Nd or Ge positions.<sup>14</sup> The temperature dependence of  $B_{hf}$  is correlated to that found in the magnetization measurements (see Figure 3). The magnetization measured using  $H = 100\text{Oe}$  showed multiple magnetic transitions with good resolution. The first transition occurs around  $450\text{K}$  and corresponds to the change from paramagnetic to antiferromagnetic phases. The second transition, from antiferromagnetic to ferromagnetic phases, is evident at  $T_t \sim 212\text{K}$  and the fourth transition, associated to the magnetic coupling of Nd atoms, becomes apparent at  $T_{Nd} \sim 25\text{K}$ . Comparing these results with those for the temperature dependence of  $B_{hf}$  from PAC measurements with  $^{111}\text{Cd}$ , one can clearly and precisely observe the paramagnetic to antiferromagnetic transition at  $T_N = 425\text{K}$ , and a slight change in the  $B_{hf}$  curve at  $T_t \sim 212\text{K}$ . The transitions observed with magnetization agree with the previously reported studies.<sup>2,11</sup> The  $T_t$  transition occurs due to Mn sublattice spins reorientation from  $c$ -axis to  $ab$ -plane with conical ferromagnetic structure on the Mn layers.<sup>2,11</sup> According to the magnetization curve around this region, this spin reorientation occurs gradually when the temperature decreases. The transition at  $25\text{K}$  is due to ferromagnetic coupling of the Nd sublattice, which contributes to slight increase in the magnetization as shown in Figure 3. PAC results with  $^{111}\text{Cd}$  probe nuclei at the saturation region in  $\text{LaMn}_2\text{Ge}_2$  presented  $B_{hf} = 19.6\text{T}$  (Ref. 12) and in  $\text{CeMn}_2\text{Ge}_2$  showed  $B_{hf} = 19.3\text{T}$ .<sup>14</sup> These results are quite similar to that of  $B_{hf} = 19.8\text{T}$  found in the present work for  $\text{NdMn}_2\text{Ge}_2$ . This similarity suggests that the contribution of Nd sublattice under  $30\text{K}$  is not observed by  $^{111}\text{Cd}$  probe or has a quite small contribution to  $B_{hf}$ , which can be understood by the fact that this probe is located at the Mn sites and is much more sensitive to the  $d_{Mn-Mn}$  distance in the intra-layer than the  $d_{Mn-Nd}$  distance in the inter-layer.

### C. PAC with $^{140}\text{Ce}$ results

The results using  $^{140}\text{Ce}$  nuclei probe allowed the precise determination of the ferromagnetic transition  $T_C$ . This is a consequence of the fact that in the antiferromagnetic phase, the magnetic structure of Mn spins induces zero hyperfine field ( $B_{hf} = 0$ ) at Nd positions, where  $^{140}\text{Ce}$  probe nuclei are located in the crystal lattice due to affinity between rare-earth elements.

Figure 4 shows a comparison between the temperature dependence of  $B_{hf}$  for  $\text{NdMn}_2\text{Ge}_2$  and  $\text{LaMn}_2\text{Ge}_2$ . This dependence presents an anomalous behavior of the Brillouin function for both samples. This behavior has been assigned to the contribution of the  $4f$  band of the Ce impurity, which is located very near the Fermi level.<sup>13</sup> For  $\text{NdMn}_2\text{Ge}_2$ , however, one can observe a yet more complex behavior in which a decrease of the  $B_{hf}$  around  $210\text{K}$  is clearly found as a result of the reorientation of the Mn spins direction from the  $c$ -axis to the  $ab$ -plane, which is also evidenced in the magnetization measurements.



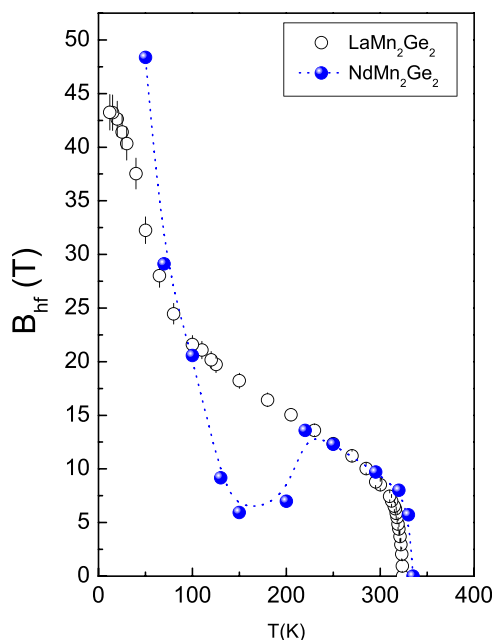


FIG. 4. Temperature dependence  $B_{hf}$  measured with  $^{140}\text{Ce}$  in  $\text{NdMn}_2\text{Ge}_2$ .

The PAC spectra in the range of temperatures where the reorientation takes place, from 200 K to 100 K, show a broad frequency distribution ( $\delta \sim 40\%$ ) not observed for spectra at other temperatures (see Figure 2). This distribution suggests that the two orientations or a mix of orientations co-exist in this region. At 70 K, (Fig. 2) the magnetic frequency is well defined again because the Mn spins are completely reoriented in ab-axis direction.  $\text{LaMn}_2\text{Ge}_2$  does not present multiple magnetic transitions following only the anomalous behavior discussed earlier.

#### IV. SUMMARY

In conclusion, measurements of magnetization and PAC spectroscopy using a combination of two probe nuclei each one located at different layers of the crystal structure of  $\text{NdMn}_2\text{Ge}_2$  were able to follow the magnetic behavior of this compound. Magnetization measurements could identify four magnetic transitions, and PAC measurements could provide details about the influence of Mn and Nd coupling on each

other. The temperature dependence of  $B_{hf}$  with  $^{140}\text{Ce}$  probe nuclei substituting the Nd positions in the crystalline lattice is more sensitive to the inter-layer interactions while  $B_{hf}$  with  $^{111}\text{Cd}$  probe nuclei at the Mn positions is sensitive to the intra-layer interactions. These two probe approach is very important when investigating the magnetic behavior of compounds that present different types of exchange interactions, such as inter-layer exchange interaction Mn-Mn and intra-layer interactions through indirect exchange that occurs between two Mn planes mediated by conduction electron polarization.<sup>9,10</sup>

#### ACKNOWLEDGMENTS

Partial financial support for this research was provided by Fapesp. B.B.S., A.W.C., R.S.F., and R.N.S. thankfully acknowledge the support provided by CNPq.

- <sup>1</sup>K. S. V. L. Narasimhan, V. U. S. Rao, R. L. Bergner, and W. E. Wallace, *J. Appl. Phys.* **46**, 4957 (1975).
- <sup>2</sup>G. J. Tomka, Cz. Kapusta, C. Ritter, and P. C. Riedi, *J. Magn. Magn. Mater.* **177**, 821–822 (1998).
- <sup>3</sup>N. P. Kolmakova, A. A. Sidorenko, and R. Z. Levitin, *Low Temp. Phys.* **28**, 653–668 (2002).
- <sup>4</sup>A. W. Carbonari, R. N. Saxena, W. Pendl, Jr., J. Mestnik-Filho, R. N. Atilli, M. Olzon-Dionysio, and S. D. de Souza, *J. Magn. Magn. Mater.* **163**, 313–321 (1996).
- <sup>5</sup>R. Dogra, A. C. Junqueira, R. N. Saxena, A. W. Carbonari, J. Mestnik-Filho, and M. Morales, *Phys. Rev. B* **63**, 224104 (2001).
- <sup>6</sup>G. A. Cabrera-Pasca, A. W. Carbonari, B. Bosch-Santos, J. Mestnik-Filho, and R. N. Saxena, *J. Phys.: Condens. Matter* **24**, 416002 (2012).
- <sup>7</sup>Y. Q. Chen, J. Luo, J. K. Liang, J. B. Li, and G. H. Rao, *J. Alloys Compd.* **489**, 13 (2010).
- <sup>8</sup>T. Shigeoka, N. Iwata, H. Jujii, and T. Okamoto, *J. Magn. Magn. Mater.* **53**, 83 (1985).
- <sup>9</sup>S. A. Granovsky, I. Yu. Gaidukova, M. Doerr, M. Loewenhaupt, A. S. Markosyan, and C. Ritter, *Physica B* **391**, 79–87 (2007).
- <sup>10</sup>E. V. Sampathkumaran, L. C. Gupta, R. Vijayaraghavan, L. D. Khoi, and P. Veillet, *J. Phys. F: Met. Phys.* **12**, 1039–1043 (1982).
- <sup>11</sup>I. Nowik, Y. Levi, I. Felner, and E. R. Bauminger, *J. Magn. Magn. Mater.* **147**, 373–384 (1995).
- <sup>12</sup>B. Bosch-Santos, A. W. Carbonari, G. A. Cabrera-Pasca, and R. N. Saxena, *J. Appl. Phys.* **115**, 17E124 (2014).
- <sup>13</sup>B. Bosch-Santos, A. W. Carbonari, G. A. Cabrera-Pasca, M. S. Costa, and R. N. Saxena, *J. Appl. Phys.* **113**, 17E124 (2013).
- <sup>14</sup>A. W. Carbonari, J. Mestnik-Filho, R. N. Saxena, and M. V. Lalić, *Phys. Rev. B* **69**, 144425 (2004).